Title: *Repeat short-interval fires put carbon storage at risk in Interior Alaska via cumulative combustion of soil carbon*

Authors: Katherine Hayes[1], Melissa Lucash[2], Kristin Olson[3], Brian Buma[1]

[1]Department of Integrative Biology, University of Colorado Denver

[2]Department of Geography, University of Oregon

[3]Department of Biology and Wildlife, University of Alaska Fairbanks

Corresponding author: Katherine.hayes@ucdenver.edu

Abstract (269/300)

Fire regimes alter the distribution, accumulation, and stability of carbon stocks across multiple spatial and temporal scales, especially in boreal ecosystems, globally important storehouses of terrestrial carbon stocks. Increasing temperatures and snow-free times have resulted in a greater frequency of short-interval fires in Interior Alaska (fires occurring within 50 years or less from proceeding fires), which depart from historic fire-interval norms, where fires were historically infrequent and severe, occurring every 150-300 years. Increasing fire frequency causes shifts in forest structure and composition that impact carbon storage, but the extent, strength and mechanisms of those effects remain unclear: fast-growing broadleaf species may lead to greater aboveground biomass in reburned stands, but the cumulative severity of multiple-fires may burn into carbon-rich soil organic layers. Here, we quantify aboveground and soil carbon in boreal black spruce (*Picea mariana*) stands that have burned once, twice or three times in the last 70 years in short intervals (>50 years). We quantified the effects of cumulative severity, stand structure and composition on both aboveground and soil carbon in an upland and lowland stand. Total carbon in reburned stands declined with additional fires, even with increases in tree density of faster-growing deciduous trees. Cumulative severity had the largest effect on aboveground

biomass and soil carbon stocks in both sites but particularly uplands, indicating the effects of continued reburning on carbon storage may differ across topographic position. This work expands our understanding of future carbon dynamics in the boreal forest, particularly in the context of new emerging short-interval fire dynamics and contributes to a larger body of knowledge on the impacts of continued disturbances on carbon storage.

Keywords: Carbon, boreal, short-interval fires, reburning, fire

Introduction

Boreal forests are a globally-important storehouse of carbon; as much as 30% of the world's terrestrial carbon stocks are stored within the forest floor and soil (IPCC 2021). In interior Alaska, fire drives the distribution, accumulation, and stability of C across spatial and temporal scales (Kasischke and Stocks 2012). However, changing climate and wildfire regimes may threaten boreal carbon stocks at regional scales (Walker et al. 2019; Dieleman et al. 2020) with the potential to exacerbate global climate change.

Soil carbon is the dominant form of carbon in the boreal forest – limited aboveground productivity and cold and/or anaerobic soil conditions promote permafrost and the accumulation of "legacy" carbon (carbon that persists across fire events, Walker et al. 2019). Post-fire soil carbon may reaccumulate via several mechanisms, including increased input of litter from regenerating biomass, the production of pyrogenic carbon or physical shifts in porosity, pH and stability driven by combustion (Pellegrini et al. 2022). Thus, after a single fire event, soil carbon recovers relatively quickly in black spruce stands, reaccumulationg X-X inches per year (CITE). Consequently, soil carbon inputs from litter or pyrogenic carbon balance soil carbon losses from combustion within 7 to 15 years after fire (O'Neill, Richter, and Kasischke 2006; Shabaga et al. 2022). However, [place for discussing soil depth??] fires that reburn previous fire perimeters within short intervals (repeat fires or reburns) can burn more deeply into organic soils, releasing not only larger amounts of carbon, but combusting legacy carbon (Walker et al. 2019) and increasing the rate of permafrost thaw due to thin (or eliminated) insulating organic layers.

Aboveground carbon is more dynamic and strongly mediates how changes in the fire regime will alter boreal composition and carbon stocks in the future, both above and belowground. Black spruce forests cover nearly 45% of all forested area in Alaska (Calef et al.

2005; van Cleve et al. 1983), and store the greatest amount of carbon relative to other forest types in the region (Johnson and Kern 2002). Thick soil organic layers associated with black spruce forests prevent seed germination of broadleaf species whose smaller seeds often can't survive in moss layers as long as larger black spruce seeds (Johnstone and Chapin 2006), maintaining "ecological inertia" at the landscape scale (Harden et al. 2006). Coniferous forests regenerate strongly after a fire via serotinous cones and dominated the regionsince the late Holocene (Hoecker et al. 2020). However, a single reburn (a second fire that burns shortly after the first) can produce mixed regeneration stands, as slow growing, dispersal-limited spruce are killed prior to maturity, particularly in the subsequent first or second decades after fire. Continued reburning (multiple short-interval fires) can convert dense black spruce stands into open broadleaf stands (Hayes and Buma 2021).

Fast-growing deciduous species produce greater overall aboveground carbon compared to black spruce 20 to 60 years after fire events (Alexander et al. 2012), outweighing losses in carbon from soil consumption (Mack et al. 2021). Over a third of Alaskan black spruce stands are considered susceptible to shifting to deciduous dominance via reburn-conversion (Kurkowski et al. 2008), so resolving the question of whether aboveground carbon pool increases will offset losses in belowground carbon pools under novel reburning conditions is critical to understanding the future of carbon cycling across the North American boreal.

This study quantifies aboveground and soil carbon in reburned stands and investigates the role of forest composition, forest structure, and cumulative fire severity in altering above and belowground carbon pools. We ask the following questions: 1) what is the impact of continued reburning on carbon stocks (aboveground live, soil, dead, and total) in Interior Alaska? and 2)

how do site-level differences in tree density, forest composition and cumulative severity correlate with carbon storage in reburned uplands and lowlands?

Methods

Figure 1. Map of Study Sites [adding after defense]

Study design

The study was conducted at two locations in Interior Alaska that have experienced 0-3 fires at intervals of < 30 years (most recent burn in all plots was 2004 or 2005). Sites were originally dominated by mature black spruce stands, confirmed via aerial photography and remote sensing (Hayes and Buma 2021), and contain a mosaic of overlapping fire perimeters from 1953 to 2005 allowing for opportunistic, spatially-constrained sampling of differing fire frequencies in areas with the same initial composition. We established fifty 400 m^2 plots in summer field seasons in 2018 and 2019, a minimum of 90 meters apart (Fig. 1). Reburned plots (n = 42) were established a minimum of 100 meters from burn perimeters, outside the dispersal distance of black spruce (one to two times the height of the seed tree, ~ 50 m, LeBarron 1939). All burned stands experienced complete aboveground mortality during each fire. We also established a total of eight unburned reference plots within bordering unburned black spruce remnant forests.

We cored snags of each species represented at each plot to confirm the fire history at reburned plots and ensure no trees survived prior fires. We also cored to estimate stand age of mature reference plots. Cores were mounted, sanded, and then imaged using ImageJ to visualize fine rings (Schneider, Rasband, and Eliceiri 2012).

Estimating Aboveground Carbon

We estimated aboveground carbon in the field by measuring tree and shrub diameters above diameter at breast height (DBH, 1.37 m). In sites where density prevented sampling the full 400-m^2, we sampled across a randomly selected 100-m^2 subplot and scaled up. We used regionally developed, species-specific allometric equations (Bond-Lamberty, Wang, and Gower 2002) to estimate total aboveground carbon within live and dead trees (see specifics in Appendix 1: Table S1). We were unable to locate local allometric equations for *Alnus viridis crispa* based on DBH and relied on regional equations for *Alnus viridis sinuata* instead (Binkley et al. 1984).

To account for carbon stored in dead or downed trees and debris, we measured downed woody debris (DWD, dead wood lying or standing below <45-degree angle) using two 28-m transects radiating from the center of each plot and converted DWD field data into estimates of mass per area (grams per meter) following Brown (2003).

To estimate herbaceous and shrub understory plant biomass, we harvested all material in 10 randomly selected 1m^2 subplots at each plot and dried samples in paper bags at 50° C. We scaled the resulting dry weight to an estimate of understory biomass in grams per square meter.

Estimating Soil Carbon

We took soil cores at the corners and the center of each plot (n = 5 per plot) using a 15-cm depth volumetric sampler. We recorded organic layer depth and sampled organic and mineral soil layers separately, and calculated bulk density for each. Mineral soil samples were sieved into two size classes (>2 mm and <2 mm) and homogenized in plastic bags. We ground soils using a roller mill, before combusting in an Costech 8020 Elemental Analyzer to estimate the % carbon of each sample. We calculated total carbon contained within organic and mineral soil horizons as

the product of each horizon's depth, bulk density, and carbon percent, and scaled estimates to grams per square meter.

Data Analysis

To quantify the impact of reburning on carbon and to test for an interactive role of site, we directly compared major pools (aboveground, soil, DWD, and overall total carbon) across fire histories. We then used hierarchical Bayesian models to estimate the strength of correlation between observed carbon and specific, plot level covariates (Kéry and Royle 2020). To explore whether the direct and indirect effects of continued reburning (shifts in forest structure, composition, and soil organic layer) were good predictors of carbon storage in biomass and soil carbon, we used two hierarchical log-normally distributed multivariate Bayesian regression models to compare effect sizes of site-level forest structure, composition, and cumulative severity on (1) live aboveground biomass and (2) soil carbon. The model structure was the same for both response variables, with a slight difference in modeled sources of measurement error (see below):

$$\log(\mu_{ij}) = \alpha_j + \beta 1(Density) *_{ij} + \beta 2(Deciduous\ BA) x_{ij} + \beta 3(SOL) * x_{ij} + \varepsilon_i$$

where μ_{ij} represents the mean carbon in plot i within a given site, α_j represents the intercept, β represents the slope coefficients of each predictor variable and ε_i represents a normally distributed error term. We used the density of trees (trees per meter^2) to represent forest structure, given the importance of tree density as a mechanism in Mack et al. 2021. Also, the short and consistent time since last burn across all sites results in minimal variation in height or other similar metrics of structure. To represent the shift in species composition from conifer to deciduous, we used the sum of the basal area of deciduous species (basal area per m^2). We picked soil organic layer depth (averaged across plot, in cm) to represent cumulative burn

137 severity given the role of soil consumption as a good representation of fire severity in boreal
138 forests (Harden et al. 2006). To compare effect sizes directly, we scaled each coefficient to a z
139 score between 0 and 1.

140 For both models, we used a Bayesian Markov Monte Carlo (MCMC) approach (Waller
141 et al. 2003; Hooten and Hobbs 2015) to generate posterior values of coefficients. We ran 2,500
142 iterations across 3 chains each and used trace plots to confirm that Monte Carlo chains reached
143 stationarity (presented in Appendix: Figure S2). We selected intentionally vague priors (normally
144 distributed, mean = 0, standard deviation = 1) to reflect the inherent lack of knowledge about the
145 parameters while still setting reasonable expectations.

146 Ecologists disagree whether measurement error (Holdaway et al. 2014) or allometric
147 error (Chen, Vaglio Laurin, and Valentini 2015) contribute greater uncertainty in estimates of
148 stand-level aboveground carbon. To minimize uncertainty from both sources, we relied on
149 locally-estimated species-specific allometric equations where available (Vorster et al. 2020) and
150 incorporated uncertainty associated with allometric equations explicitly within the model by
151 adding a measurement error term. We incorporated uncertainty into soil carbon estimates by
152 calculating the total uncertainty in each plot by calculating the standard deviation of the average
153 Mg of carbon per core and summing across a plot (Fourqurean et al. 2015). The total uncertainty
154 per plot was included as the error term variable in the soil carbon models. All models were built
155 using the "r2Jags" package (Su and Yajima 2012, version 1) and all analysis, model fit, and
156 selection were performed in R version 4.1.2 (R Core team 2021, *code available online*).
157 Additional information on the modeling approach and Bayesian inference used to estimate
158 coefficient effect size including the specification of prior distributions and specifics on the
159 MCMC sampler are provided in the appendix (S2).

Results

R1. How do carbon pools (overstory live and dead biomass, understory biomass, litter biomass and soil carbon) shift with continued reburning?

Total Carbon

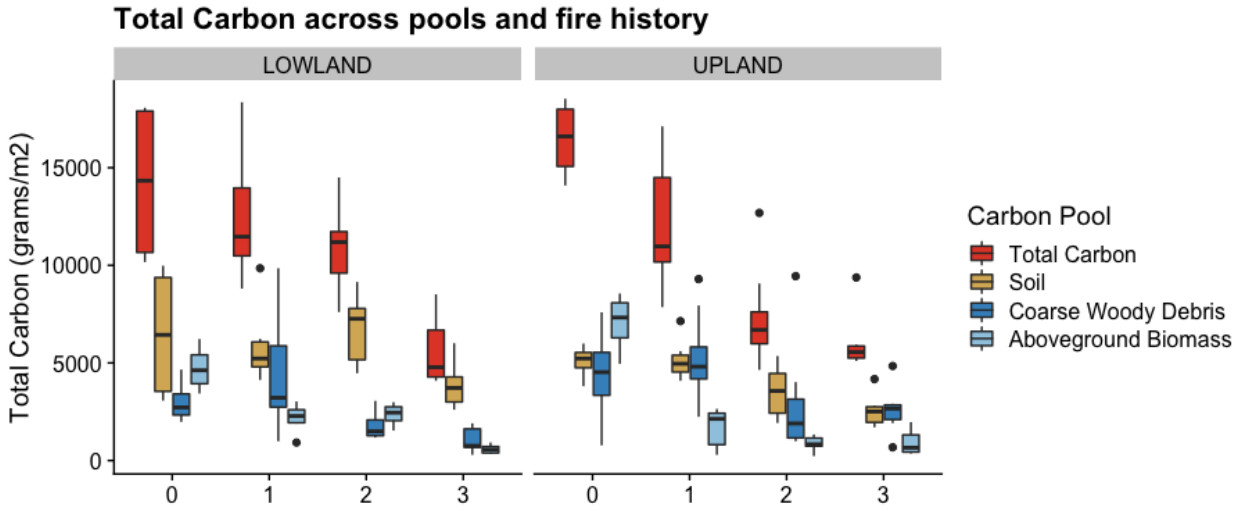

Figure 2. Total carbon (grams / m^2) across reburn history and within carbon pools. Red represents the pooled total carbon, yellow represents soil carbon ($g/m^{2)}$ and blue indicate the pools within aboveground carbon (coarse woody debris and aboveground C composed of live overstory and understory biomass). Dots represent outliers.

Total carbon declines as fire frequency increases (Fig. 2) despite the similar age of all burned plots (13-16 years since last fire); all were less than the reference stands (86-106 years since last fire; Appendix Table S2). While the lowland and upland sites contained similar amounts of total carbon prior to burning (lowlands average 14,226 g/m^2, SD 4,316; uplands average 16,456 g/m^2, SD 2,075), the total carbon in each site was compromised of different pools. Carbon in mature unburned lowland plots was primarily soil carbon (average 45.5%), while carbon in upland equivalents was primarily aboveground biomass (average 42.8% of total).

Total carbon in lowland plots declines by 12% after one fire, primarily driven by losses in soil carbon which declines by 9% on average. In comparison, carbon in upland declines by 26% - the greatest loss is in overstory biomass, which declines by an average 75%, but some of that carbon presumably transferred into coarse woody debris which increases by 17% after one fire. This differing response between sites continues with additional reburns: average total carbon in uplands declines again after two fires but remains relatively consistent in lowlands (average 12,502 g/m^2 after one fire vs average 10,910 g/m^2 after two). After three fires, average estimated total carbon declines to similar levels in both sites (7,350 g/m^2 in uplands vs 5,597 g/m^2 in lowlands).

Aboveground Biomass

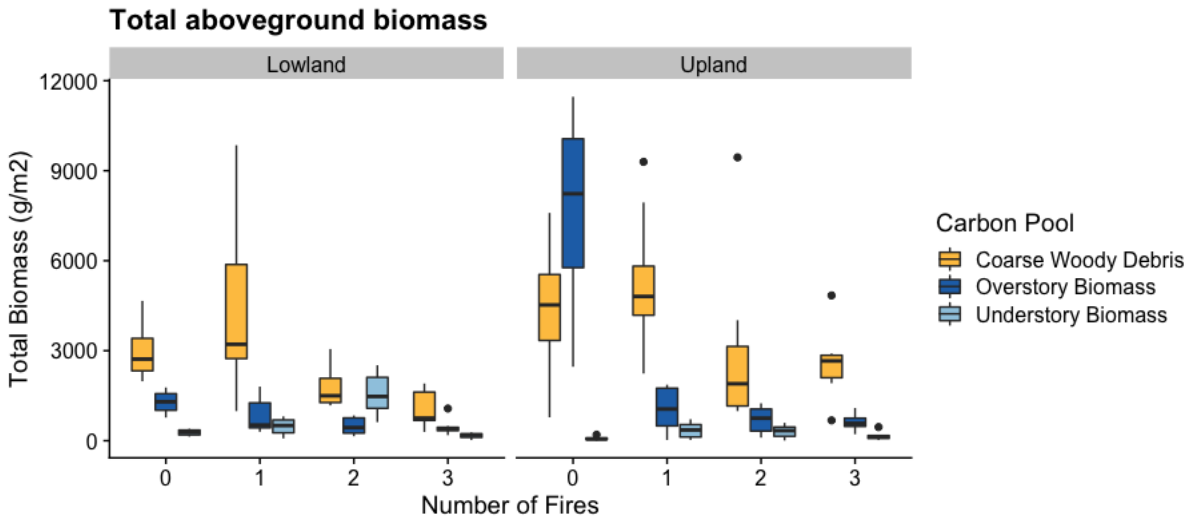

Figure 3. Aboveground Biomass (grams / m^2) across reburn history and across pools. Blue represents pooled total aboveground biomass, dark green represents overstory biomass (g/m^2) . Dots represent outliers.

Overstory biomass was the largest pool of aboveground carbon, regardless of reburning (Fig 3). Upland mature plots contained greater aboveground biomass prior to burning, due to both greater overstory and coarse woody debris biomass (Fig. 2). Coarse woody debris pools

increased in lowlands after one fire (from an average of 19% of total carbon to 45%) but was consumed further after two fires (average 2,435 g/m^2 to 1,784 g/m^2). A pulse of coarse woody debris in upland thrice-burned plots lead to greater aboveground biomass overall after three fires compared to two. Across both sites, understory biomass was the smallest carbon pool and did not appear to shift with reburning (from an average of .09% of total carbon in unburned plots to 0.46% in thrice-burned plots).

Soil Carbon

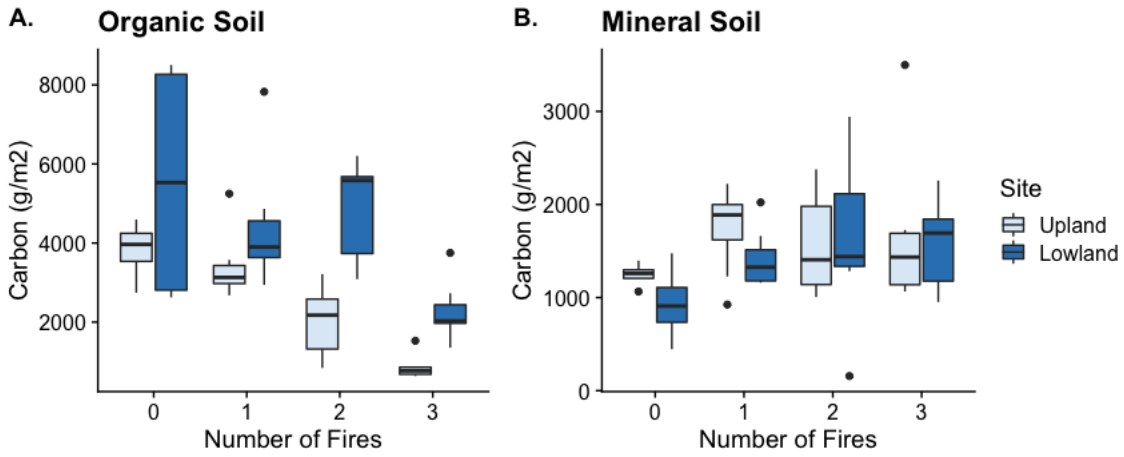

Figure 4. Carbon abundance (g/m^2) of mineral (A) and organic (B) soil layers across reburn history and between sites. Dots represent outliers.

Generally, soil organic layers contain more carbon than mineral soil. Trends in mineral and organic soil carbon pool size differ between lowland and upland sites (Fig. 4). Organic layer soil carbon declines overall within both locations with reburning, but the pace of the decline is more rapid in upland stands than lowlands (Fig. 4A). Estimates of soil organic layer carbon increase in lowlands after two fires to levels similar to mature plots (average 5,546 g/m^2 in twice-burned plots vs 4,880 g/m^2 in unburned plots). By three fires, organic soil layer is consumed altogether in some plots (soil organic layers in uplands contain twice less carbon on average than corresponding mineral soils – 874 g/m^2 in organic vs 1,707 g/m^2 in mineral).

R2. What are the effects of species composition, regeneration density, and cumulative severity on the abundance of aboveground and soil carbon in reburned stands?

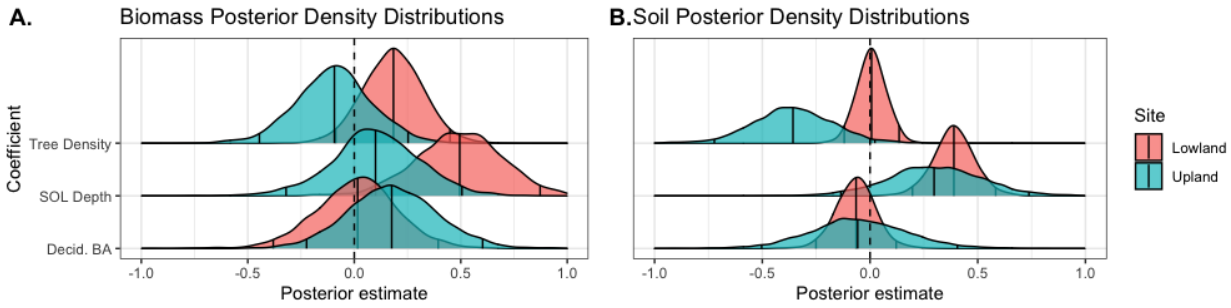

Figure 5. Posterior density distributions for site-level variable coefficients within upland and lowland field sites. Center line indicates median, ridge lines mark the edges of a 95% interval. Coefficients are z-scores, scaled to values between 0 and 1 – thus posterior estimates occur within the same range. (A) Posterior density distribution for aboveground live biomass model. (B) Posterior density distribution for soil carbon model.

The effects of tree density, soil organic layer depth and deciduous basal area on carbon followed similar trends across aboveground and soil pools but differed between sites (Fig. 6). Soil organic layer depth displayed the strongest positive effect size in both sites and both pools, but particularly in lowland plots. Tree density had negative effects on aboveground biomass and soil carbon in uplands, but no apparent effect on lowland soil carbon (median centered around 0) and a slight positive effect on lowland aboveground biomass. Deciduous basal area was not a strong predictor of either pool of lowland carbon; its strongest effect is on upland biomass, which increases as deciduous basal area increases.

Discussion

We found that both aboveground and soil carbon declined with reburning in upland and lowland stands. Tree density and deciduous basal area in reburned stands did not appear to meaningfully shape variability in carbon storage, either aboveground or in soil. Rather, soil

organic layer depth, a proxy for cumulative burn severity, had the strongest positive effect on soil and aboveground carbon, particularly in lowlands. Together, these results suggest the importance of increased fire frequency and their cumulative severity, especially of multiple fires and their potential to drive ecosystem carbon storage past documented norms.

Our mature upland stands had greater aboveground biomass than regional averages and our lowlands had lower (average aboveground biomass in 60 year-old black spruce stands is 27.7 Mg per hectare, Yarie and Billings 2002). This is in line with expectations: lowlands are generally less productive than uplands (Jafarov et al. 2013).

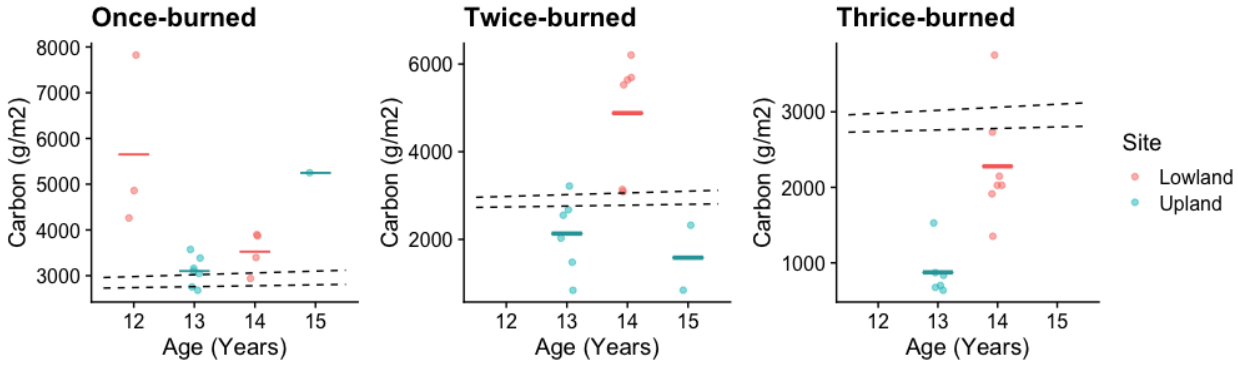

Figure 7. Observed vs predicted soil organic layer carbon across reburns. Colored horizontal averages represent averages of sites according to age in years. Dotted lines represent the range of predicted soil carbon accumulation after fire as predicted by Harden et al. 2012 and others.

Historically in the boreal, soil organic layer carbon recovers relatively quickly after fire events, accumulating roughly 20-40 grams of carbon per m^2 per year (Harden et al. 2012; Kane and Vogel 2009; O'Neill et al. 2006). Our estimates of soil organic layer carbon in reburned stands correspond well to predicted carbon accumulation rates initially (Fig. 7). However, our estimates of soil organic carbon in once-burned plots and unburned reference plots were higher than predictions, so our sites may have been relatively productive stands prior to reburning.

Upland average soil organic carbon is lower than predictions after two fires (Fig. 7B). Furthermore, when we move into burn frequencies that have not been observed before (our three-fire sequence), our observations of soil organic layer carbon depart from expectations after three fires (Fig. 7C). The difference between upland and lowland may be because of topographic differences - lowlands have poor drainage and thus greater soil moisture - greater amounts of organic layer are consumed if the layer is dryer (Kasischke and Turetsky 2006). Carbon in soil organic layers in upland plots decline past documented ranges of reburned carbon, via potentially cumulative effects of burning. While we sampled only the top 15 centimeters of mineral soil, simulations show that the bulk of carbon loses from fire in boreal soils will occur within the top meter of soil (Mekonnen et al. 2022), offsetting gains in plant carbon and transforming the ecosystem from a carbon sink to a net carbon source by 2200.

Not only are the losses in carbon crucial, the implied loss of soil organic matter itself has large implications for future boreal forest characteristics. Soil organic layers help maintain "ecological inertia" at a landscape-scale (Harden et al. 2006) by favoring black spruce regeneration. Studies like Alexander et al. (2012) and Mack et al. (2021) found that increases in the relative density, basal area and abundance of deciduous species are correlated to increases in aboveground biomass, attributing the relationship to higher annual primary productivity and faster accumulation of stemwood and bark in deciduous species compared to black spruce, but make no distinction between deciduous species. However, the impact of species-specific trends in deciduous regeneration may be important - deciduous regrowth in our reburned upland sites was primarily birch, while aspen dominated in reburned lowland plots (Hayes and Buma 2021). Both grow relatively fast after fire, but aspen is far more productive than birch (Van Cleve 1975, Viereck et al. 1986). Neither typically exist in high density pure stands in Interior Alaska

currently (birch is common in gaps, Uchtyil 1991; aspen occurs across 2 – 10% of the interior, largely in floodplains; Viereck 1975), so our understanding of their longer-term dynamics and the resulting impact on carbon is limited. Given these findings, there is the potential for divergence in carbon stocks dynamics at the deciduous species level as well in the future. Given species differences in their tolerances for differing climatic, edaphic, and hydrological conditions (Viereck et al. 1986), this could become significant as warming continues.

Because of the inherently opportunistic nature of post-disturbance sampling, this study has a few key limitations. This study samples two mosaics of fire histories, and each fire within that mosaic was shaped by various innumerable factors such as microtopography, fire weather at the scale of days or hours, or local microclimate, all factors that remain unquantifiable within the context of this study but may still all influence subsequent forest establishment and soil development. To interpret these results in the context of future carbon dynamics of the boreal ecoregion and the global carbon cycle more broadly, results from this study and from others like it (Melvin et al. 2015, Alexander et al. 2012) should be investigated in a modeling framework that allows for broader generalizations beyond these specific study sites.

Our empirical evidence shows that repeated fires enable departures from historic norms of carbon storage and cycling in interior Alaska. Future increases in fire frequency and short-interval fires, which are already observable in the rapidly warming Arctic (Buma et al. 2022), will greatly alter that dynamic. Generalizations of the results from this study and others will not be possible without estimating what proportion of the landscape will continue to burn at short intervals.

Conclusion

Declines in aboveground and soil carbon occur in reburns regardless of landscape position. Our results are consistent both with other empirical estimates of carbon storage after extreme fire and with simulations, which predict the transformation of the boreal into a net carbon source via increases in fire frequency and severity. Additionally, our study illustrates how cumulative severity of soil organic layer consumption shape carbon stocks in regenerating stands, even in historically more resilient landscape positions. Continued research into the susceptibility of the Interior to landscape-scale reburning will be critical to understanding how shifts in fire frequency will shape carbon cycling at a larger boreal scale.

Data Availability

All code used in the analyses of this paper are publicly available as a repository on GitHub (https://github.com/k8hayes/Biomass) and datasets are available on Zenodo (doi).

Acknowledgments

This research was supported by funding provided by the National Science Foundation (NSF-OPP-1903231). We thank Vishnusai Kodicherla, Kyle Martini, Pauline Allen, and Teagan Furbish for assistance in the field and to Trevor Carter, Erin Twadell, and Jason Shabaga for valuable support and advice.

References

Arias, P., Bellouin, N., Coppola, E., Jones, R., Krinner, G., Marotzke, J., Naik, V., Palmer, M., Plattner, G.K., Rogelj, J. and Rojas, M., 2021. Climate Change 2021: The Physical Science Basis. Contribution of Working Group14 I to the Sixth Assessment Report of the Intergovernmental Panel on Climate Change; Technical Summary.

Alexander, H.D., Mack, M.C., Goetz, S., Beck, P.S. and Belshe, E.F., 2012. Implications of increased deciduous cover on stand structure and aboveground carbon pools of Alaskan boreal forests. *Ecosphere*, *3*(5), pp.1-21.

Berner, L.T., Alexander, H.D., Loranty, M.M., Ganzlin, P., Mack, M.C., Davydov, S.P. and Goetz, S.J., 2015. Biomass allometry for alder, dwarf birch, and willow in boreal forest and tundra ecosystems of far northeastern Siberia and north-central Alaska. *Forest Ecology and Management*, *337*, pp.110-118.

Binkley, D., Lousier, J.D. and Cromack Jr, K., 1984. Ecosystem effects of Sitka alder in a Douglas-fir plantation. *Forest Science*, *30*(1), pp.26-35.

Bond-Lamberty, B., Wang, C. and Gower, S.T., 2002. Aboveground and belowground biomass and sapwood area allometric equations for six boreal tree species of northern Manitoba. *Canadian Journal of Forest Research*, *32*(8), pp.1441-1450.

Buma, B., Hayes, K., Weiss, S. and Lucash, M., 2022. Short-interval fires increasing in the Alaskan boreal forest as fire self-regulation decays across forest types. *Scientific reports*, *12*(1), pp.1-10.

Brown, J.K., 2003. *Coarse woody debris: managing benefits and fire hazard in the recovering forest*. US Department of Agriculture, Forest Service, Rocky Mountain Research Station.

Calef, M.P., David McGuire, A., Epstein, H.E., Scott Rupp, T. and Shugart, H.H., 2005. Analysis of vegetation distribution in Interior Alaska and sensitivity to climate change using a logistic regression approach. *Journal of Biogeography*, *32*(5), pp.863-878.

Chen, Q., Laurin, G.V. and Valentini, R., 2015. Uncertainty of remotely sensed aboveground biomass over an African tropical forest: Propagating errors from trees to plots to pixels. *Remote Sensing of Environment*, *160*, pp.134-143.

Dieleman, C.M., Rogers, B.M., Potter, S., Veraverbeke, S., Johnstone, J.F., Laflamme, J., Solvik, K., Walker, X.J., Mack, M.C. and Turetsky, M.R., 2020. Wildfire combustion and carbon stocks in the southern Canadian boreal forest: Implications for a warming world. *Global change biology*, *26*(11), pp.6062-6079.

Fourqurean, J., Johnson, B., Kauffman, J.B., Kennedy, H., Lovelock, C., Alongi, D.M., Cifuentes, M., Copertino, M., Crooks, S., Duarte, C. and Fortes, M., 2015. Field sampling of soil carbon pools in coastal ecosystems.

Harden, J.W., Manies, K.L., Turetsky, M.R. and Neff, J.C., 2006. Effects of wildfire and permafrost on soil organic matter and soil climate in interior Alaska. *Global Change Biology*, *12*(12), pp.2391-2403.

Harden, J.W., Manies, K.L., O'Donnell, J., Johnson, K., Frolking, S. and Fan, Z., 2012. Spatiotemporal analysis of black spruce forest soils and implications for the fate of C. *Journal of Geophysical Research: Biogeosciences*, *117*(G1).

Hayes, K. and Buma, B., 2021. Effects of short-interval disturbances continue to accumulate, overwhelming variability in local resilience. *Ecosphere*, *12*(3), p.e03379.

Hoecker, T.J., Higuera, P.E., Kelly, R. and Hu, F.S., 2020. Arctic and boreal paleofire records reveal drivers of fire activity and departures from Holocene variability. *Ecology*, *101*(9), p.e03096.

Holdaway, R.J., McNeill, S.J., Mason, N.W. and Carswell, F.E., 2014. Propagating uncertainty in plot-based estimates of forest carbon stock and carbon stock change. *Ecosystems*, *17*(4), pp.627-640.

Hooten, M.B. and Hobbs, N.T., 2015. A guide to Bayesian model selection for ecologists. *Ecological monographs*, *85*(1), pp.3-28.

Jafarov, E.E., Romanovsky, V.E., Genet, H., McGuire, A.D. and Marchenko, S.S., 2013. The effects of fire on the thermal stability of permafrost in lowland and upland black spruce forests of interior Alaska in a changing climate. *Environmental Research Letters*, *8*(3), p.035030.

Jayen, K., Leduc, A. and Bergeron, Y., 2006. Effect of fire severity on regeneration success in the boreal forest of northwest Quebec, Canada. *Ecoscience*, *13*(2), pp.143-151.

Johnston, W.F., 1971. *Management guide for the black spruce type in the lake states* (Vol. 64). North Central Forest Experiment Station, Forest Service, US Department of Agriculture.

Johnstone, J. F., and F. S. Chapin. 2006. Effects of soil burn severity on post-fire tree recruitment in boreal forest. *Ecosystems* 9(1): 14-31.

Johnson, M.G. and Kern, J.S., 2002. Quantifying the organic carbon held in forested soils of the United States and Puerto Rico. In *The potential of US forest soils to sequester carbon and mitigate the greenhouse effect* (pp. 47-72). CRC press.

Kane, E.S. and Vogel, J.G., 2009. Patterns of total ecosystem carbon storage with changes in soil temperature in boreal black spruce forests. *Ecosystems*, *12*(2), pp.322-335.

Kasischke, E.S. and Turetsky, M.R., 2006. Recent changes in the fire regime across the North American boreal region—Spatial and temporal patterns of burning across Canada and Alaska. *Geophysical research letters*, *33*(9).

Kasischke, E.S. and Stocks, B.J. eds., 2012. *Fire, climate change, and carbon cycling in the boreal forest* (Vol. 138). Springer Science & Business Media.

Kéry, M. and Royle, J.A., 2020. *Applied Hierarchical Modeling in Ecology: Analysis of distribution, abundance and species richness in R and BUGS: Volume 2: Dynamic and Advanced Models*. Academic Press.

Kurkowski, T. A., et al. 2008. Relative importance of different secondary successional pathways in an Alaskan boreal forest. *Canadian Journal of Forest Research* 38(7): 1911-1923.

LeBarron, R.K., 1939. The role of forest fires in the reproduction of black spruce. *Journal of the Minnesota Academy of Science*, *7*(1), pp.10-14.

Mack, M.C., Walker, X.J., Johnstone, J.F., Alexander, H.D., Melvin, A.M., Jean, M. and Miller, S.N., 2021. Carbon loss from boreal forest wildfires offset by increased dominance of deciduous trees. *Science*, *372*(6539), pp.280-283.

Mekonnen, Z.A., Riley, W.J., Randerson, J.T., Shirley, I.A., Bouskill, N.J. and Grant, R.F., 2022. Wildfire exacerbates high-latitude soil carbon losses from climate warming. *Environmental Research Letters*, *17*(9), p.094037.

Melvin, A.M., Mack, M.C., Johnstone, J.F., David McGuire, A., Genet, H. and Schuur, E.A., 2015. Differences in ecosystem carbon distribution and nutrient cycling linked to forest tree species composition in a mid-successional boreal forest. *Ecosystems*, *18*(8), pp.1472-1488.

O'Neill, K.P., Richter, D.D. and Kasischke, E.S., 2006. Succession-driven changes in soil respiration following fire in black spruce stands of interior Alaska. *Biogeochemistry*, *80*(1), pp.1-20.

Pan, Y., Birdsey, R.A., Fang, J., Houghton, R., Kauppi, P.E., Kurz, W.A., Phillips, O.L., Shvidenko, A., Lewis, S.L., Canadell, J.G. and Ciais, P., 2011. A large and persistent carbon sink in the world's forests. *Science*, 333(6045), pp.988-993.

Pellegrini, A.F., Harden, J., Georgiou, K., Hemes, K.S., Malhotra, A., Nolan, C.J. and Jackson, R.B., 2022. Fire effects on the persistence of soil organic matter and long-term carbon storage. *Nature Geoscience*, *15*(1), pp.5-13.

R Core Team (2021). R: A language and environment for statistical computing. R Foundation for Statistical Computing, Vienna, Austria. URL https://www.R-project.org/.

Schneider, C.A., Rasband, W.S. and Eliceiri, K.W., 2012. NIH Image to ImageJ: 25 years of image analysis. *Nature methods*, *9*(7), pp.671-675.

Shabaga, J.A., Bracho, R., Klockow, P.A., Lucash, M.S. and Vogel, J.G., 2022. Shortened Fire Intervals Stimulate Carbon Losses from Heterotrophic Respiration and Reduce Understorey Plant Productivity in Boreal Forests. *Ecosystems*, pp.1-26.

Su, Yu-Sung and Yajima, Masanao. 2021. "R2jags: Using R to Run 'JAGS'. R package version 0.7-1. https://CRAN.R-project.org/package=R2jags

Thompson Hobbs, N., and Mevin B. Hooten. 2015. *Bayesian Models: A Statistical Primer for Ecologists*. Princeton University Press.

Van Cleve, K., Dyrness, C.T., Viereck, L.A., Fox, J., Chapin III, F.S. and Oechel, W., 1983. Taiga ecosystems in interior Alaska. *Bioscience*, *33*(1), pp.39-44

Viereck, L.A., 1975. Forest ecology of the Alaska taiga.

Viereck, L.A., Cleve, K.V. and Dyrness, C.T., 1986. Forest ecosystem distribution in the taiga environment. In *Forest ecosystems in the Alaskan taiga* (pp. 22-43). Springer, New York, NY.

Vorster, A.G., Evangelista, P.H., Stovall, A.E. and Ex, S., 2020. Variability and uncertainty in forest biomass estimates from the tree to landscape scale: The role of allometric equations. *Carbon balance and management*, *15*(1), pp.1-20.

Walker, X.J., Baltzer, J.L., Cumming, S.G., Day, N.J., Ebert, C., Goetz, S., Johnstone, J.F., Potter, S., Rogers, B.M., Schuur, E.A. and Turetsky, M.R., 2019. Increasing wildfires threaten historic carbon sink of boreal forest soils. *Nature*, *572*(7770), pp.520-523.

Waller, L.A., Smith, D., Childs, J.E. and Real, L.A., 2003. Monte Carlo assessments of goodness-of-fit for ecological simulation models. *Ecological Modelling*, *164*(1), pp.49-63.

Yarie, J. and Billings, S., 2002. Carbon balance of the taiga forest within Alaska: present and future. *Canadian Journal of Forest Research*, *32*(5), pp.757-767.

***Journal* Supporting Information**

Article Title:

Authors: Katherine Hayes, Melissa Lucash, Brian Buma

429

S1. Allometric Equations

Table S1. Allometric equations used to calculate aboveground biomass.

Species	Source	Comp.	Equation	R2	Their DBH range	Our DBH range (CM)	Error
Populus tremuloides	Bond-Lamberty et al. 2002	Total	$Log_{10}Y = 2.614 + 0.852*(log_{10}DBH)$	0.99	0.3-23.7	0.1 – 6.5	MSE 0.016
Populus balsamifera	Byrd 2013	Total	$y = 0.261e^{0.0591*DBH}$	0.86	AV 2.77	1.3 – 2.3	
Betula neoalaskana	Bond-Lamberty et al. 2002	Total	$Log_{10}Y = 2.462 + 1.095*(log_{10}DBH)$	0.66	0.3-0.7	0.1 – 23.5	MSE 0.012
Picea Mariana	Bond-Lamberty et al. 2002	Total	$Log_{10}Y = 3.011 + 1.202*(log_{10}DBH) + -.01(AGE) + 0.972(Log_{10}DBH*AGE)$	0.97	0.5-17	0.1 - 20	MSE 0.021
Salix	Bond-Lamberty et al. 2002	Total	$Log_{10}Y = 2.481 + 1.19(log_{10}DBH)$	0.54	0.3-1	0.1 – 8.1	MSE 0.043
Alnus	Binkley et al. 1984	Stem		0.88		0.2 – 4.5	SE 0.276
		Leaves		0.88			SE 0.127

S2. Tree ring core results

We took tree-ring cores at each plot to estimate the age of mature (unburned) stands and to provide additional estimates of the age of reburned stands. Not all reburned stands contained individuals large enough to take a tree core (marked "No sample" in the table below).

Table S2. Results of tree-ring cores taken at each plot. Age is represented in years – we report the oldest date obtained from dating tree cores, as well as the median date. We present both next to the confirmed age of the stand based on fire history obtained from aerial photographs and remote sensing.

Site	Burn History	Plot	n	Max Age	Median Age	Confirmed age
Upland	Mature	10_0	11	78	86	
		11_0	10	78	87	
		44_0	11	79	83	
		58_0	19	75	87	
	1 fire	42_1	1	16	16	16
		12_1	7	7	11	14
		41_1	3	15	27	
		48_1	4	9	10	
		50_1		No sample		
		52_1	2	11	11	
		64_1		No sample		
		65_1		No sample		
	2 fires	40_2	3	16	18	16
		32_2	6	13	16	
		39_2	6	11.5	14	14
		16_2	4	10	12	
		47_2		No sample		
		56_2	4	7.5	10	
		57_2	6	9	14	
		8_2	6	9	13	
	3 fires	14_3	3	7	11	14
		15_3	2	11	14	
		37_3	4	8	15	
		54_3	4	9	10	
		55_3	1	52	52	
		7_3	4	67	9	
Lowland	Unburned	1_0	4	81	93	
		31_0	3	61	106	
		6_0	7	80	84	
		9_0	6	83	88	
	1 fire	18_1	1	15	15	15
		33_1	1	15	15	
		28_1	1	15	15	
		29_1	2	8	10	

		20_1	1	13	13	13
		36_1	1	13	13	
		5_1	1	15	15	
	Two fires	19_2	1	66	66	15
		26_2	2	9	9	
		27_2	1	66	66	
		3_2	4	10	12	
		34_2	1	62	62	
		4_2		No sample		
	Three fires	17_3	1	62	62	15
		2_3	3	8	9	
		22_3	1	62	62	
		23_3	4	9	11	
		24_3	3	12	15	
		25_3	3	12	13	
		35_3	2	12.5	14	

S3. Bayesian Models

Model Specification

Bayesian Model Implementation

The Bayesian hierarchical model is completed by specifying prior distributions for model parameters. Those include …. We used Markov Monte Carlo (MCMC) to sample from the joint posterior distribution for all model parameters ()

We assigned normal priors for all regression coefficients within the X and X models. Specifically …

We used a Metropolis-within-Gibbs Markov chain Monte Carlo (MCMC) algorithm to sample from the joint posterior distribution for all model parameters () using the package "R2Jags" (Su and Yajima 2021, version 07.1). For each model, we ran 3 chains across 2,500 iterations following a burn-in of 100 samples. We assessed convergence visually using traceplots (included below in Figure S ##).

Figure S#. Traceplots from model of biomass as a function of fire modified by site.

Inferences

- Display posteriors such that it could be used as priors in future study
    - Table with means, medians, variances/sd, quantiles of parameters
    - Including whether they have skewed / multimodal densities

Table S1. Posterior Median values (and 95 percent credible intervals) for site-specific effect coefficients and plot- and site-level variances for the Upland and Lowland site.

Model	Parameter	Median	95						
Biomass	Intercept								
	Coefficient								
Soil C	Intercept								
	Coefficient								

Appropriate inferences from 1 + model

- Look at chapter 9 for specifics
- Go beyond AIC weights